JOURNAL OF THERMOPHYSICS AND HEAT TRANSFER
Vol. 14, No. 2, April–June 2000

Thermal Analysis and Design of an Advanced Space Suit

Anthony B. Campbell,* Jonathan D. French,* Satish S. Nair,† and John B. Miles‡
University of Missouri, Columbia, Missouri 65211
and
Chin H. Lin§
NASA Johnson Space Center, Houston, Texas 77058

The thermal dynamics and design of an advanced space suit are considered. A transient model of the advanced space suit design has been developed and implemented using MATLAB®/Simulink, to help with sizing, with design evaluation, and with the development of an automatic thermal comfort control strategy. The model is described and the thermal characteristics of the advanced space suit are investigated including various parametric design studies. The steady-state performance envelope for the advanced space suit is defined in terms of the thermal environment and human metabolic rate and the transient response of the human-suit–minimum consumables portable life support system is analyzed.

Nomenclature

$\dot{Q}_{LCG}$ = liquid cooling garment (LCG) heat loss
$\dot{Q}_{lat}$ = latent heat loss
$\dot{Q}_{met}$ = metabolic heat addition
$\dot{Q}_{resp}$ = respiratory heat loss
$\dot{Q}_{shiv}$ = shivering heat addition
Q_{stor} = total body heat storage
$\dot{Q}_{suit}$ = suit heat loss
$\dot{Q}_{VG}$ = vent gas heat loss
$T_{in,dewpt}$ = VG inlet dew point
$T_{in,lcg}$ = LCG inlet temperature
$T_{in,vg}$ = ventilation garment (VG) inlet temperature
T_{so} = outer suit temperature

I. Introduction

THE increased demands of extravehicular activity (EVA) for the International Space Station (ISS) assembly and maintenance along with planned lunar and Martian missions necessitate the development of a new advanced space suit and portable life support system (PLSS). NASA is developing an advanced space suit, the minimum consumables PLSS (MPLSS), for possible ISS, lunar, and Martian missions.[1] The requirements for the advanced space suit[2] are derived primarily from the Martian mission because these are the most demanding. The Martian environment can vary from −123 to 20°C (−190 to 70°F) with sustained wind speeds as high as 15 m/s (49 ft/s).

The MPLSS system diagram can be seen in Fig. 1 along with the baseline design's heat loads. The MPLSS, like the current Shuttle PLSS,[3–5] contains a water cooling loop (WCL) and a ventilation loop (VL). The WCL will remove the majority (60–80%) of the heat from the body via a liquid cooled garment (LCG). This heat will then be rejected to space via a radiator unit and a water boiler. The radiator is the primary heat rejection source with the water boiler being the secondary or topping unit for heat rejection. The WCL also removes heat from the VL via the trim cooler. A comfort heater has been included in the WCL to help with the cold discomfort problems seen in the Space Shuttle suit. The temperature of the water entering the LCG is controlled by the temperature control valve (TCV) positions for the radiator and water boiler, as well as the comfort heater input. The VL removes a smaller portion (20–40%) of the astronaut's metabolic heat load through sensible and latent heat transfer in the suit. The VL removes carbon dioxide and moisture from the suit and expends them to space via the dual bed scrubber. The VL then supplies oxygen at a comfortable temperature and humidity after passing through a fan and trim cooler.

The objectives of this paper are twofold. The first is to provide a description and system level overview of the thermal control technologies associated with a space suit system. The second is to discuss the thermal dynamic characteristics of the MPLSS using a detailed simulation model, the development of which is also described. The dynamic simulation model serves as a testbed for a host of studies including thermal design, parametric analyses, development of reduced-order models, and control design.

As mentioned, a transient thermal model of the MPLSS has been developed so that system performance and thermal comfort can be evaluated for different mission profiles and environmental conditions. Environmental profiles for temperature, wind speed (on Mars), and solar flux, as well as metabolic profiles for varying activities, can be prescribed to evaluate system performance. The design environmental and metabolic rate profiles used in this study are shown in Fig. 2. The model will be used to investigate component sizing, PLSS configuration, and thermal comfort control. The model was built with a modular structure so that alternative components can be added for evaluating design modifications. Components can easily be interchanged with other PLSS models[3,6] so that hybrid PLSS configurations can be analyzed. The MPLSS design and operational restrictions or remedies, such as donning and doffing of outer garments, can also be analyzed with the model. Section II lists the dynamic model development issues. Section III discusses the baseline design performance and results of parametric studies. The operating envelope and dynamic characteristics of subsystems and the overall system are discussed in Sec. IV. The results and the important insights are reported next, followed by conclusions.

II. Model Description

The MPLSS model is developed and implemented in a modular form using MATLAB®/Simulink software. The main MPLSS model window is shown in Fig. 3. Each component block is a submodel representing the thermal dynamic equations for the component. Wide vector lines represent the flowing fluid properties in the WCL and VL. The WCL vectors represent temperature, pressure,

Received 9 June 1999; revision received 7 December 1999; accepted for publication 17 December 1999.

*Ph.D. Student, Department of Mechanical and Aerospace Engineering.
†Associate Professor, Department of Mechanical and Aerospace Engineering.
‡Emeritus Professor, Department of Mechanical and Aerospace Engineering.
§Branch Chief, Crew and Thermal Systems Division, Systems Design and Analysis Branch.

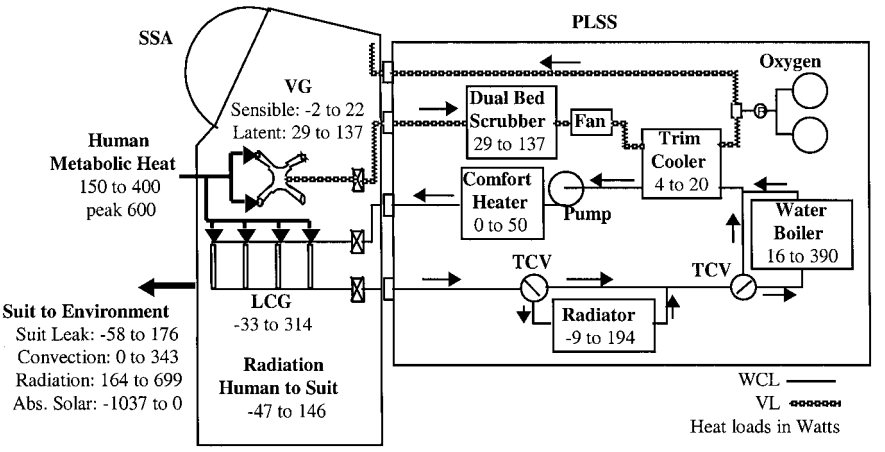

Fig. 1 MPLSS system schematic with heat loads.

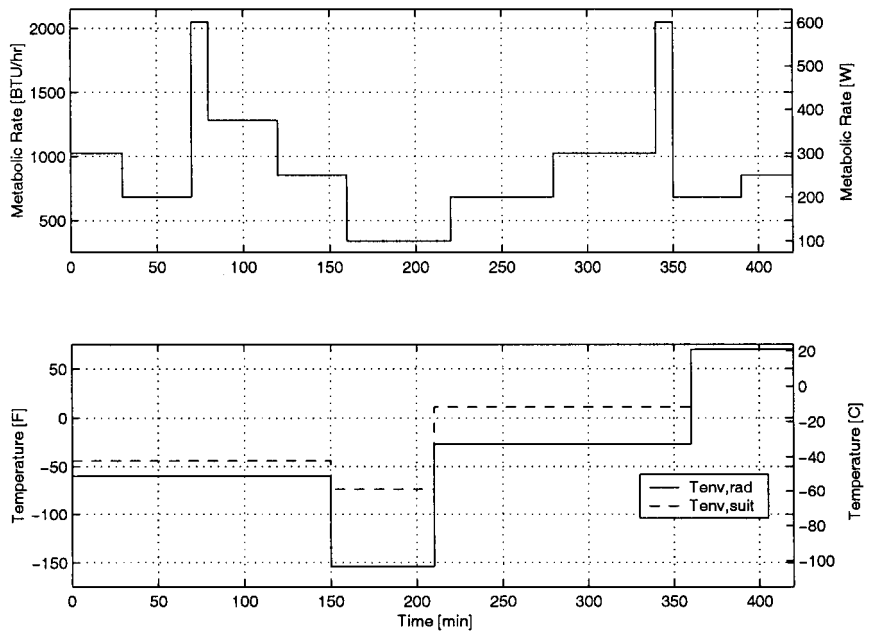

Fig. 2 Design metabolic rate and environmental profiles.

and mass flow rate. The VL vectors represent temperature, pressure, mass flow rate, and dew point. A lumped parameter approach is used to model the various components and the human. With this approach, the complete model currently consists of 26 nodes for the PLSS, 41 nodes for the human, 35 nodes for the suit, and two nodes for the thermal environment.

A. MPLSS Components

The general equation for a fluid node in the model is given by

$$m_i c_{p,i} \frac{\mathrm{d}T_i}{\mathrm{d}t} = q_{\mathrm{conv},i} + \dot{m}_i c_{p,i}(T_{\mathrm{in},i} - T_i) \tag{1}$$

where $q_{\mathrm{conv},i}$ is the convective heat transfer with the component and m_i, $c_{p,i}$, and T_i are the mass, specific heat, and temperature of fluid node i. The general equation for a structure node I in the model is given by

$$m_i c_{p,i} \frac{\mathrm{d}T_i}{\mathrm{d}t} = \sum_j q_{\mathrm{cond},ij} + \sum_k q_{\mathrm{conv},ik} + \sum_l q_{\mathrm{rad},il} \tag{2}$$

where $q_{\mathrm{cond},ij}$, $q_{\mathrm{conv},ij}$, and $q_{\mathrm{rad},il}$ are the conductive, convective, and radiative heat transfer with the surrounding nodes. All components are assumed to be insulated from each other with the exception of WCL and VL flow interactions. This is in agreement with recent structural designs developed by NASA (private communications, M. Rouen, NASA Johnson Space Center, 1999) and is significant as was seen with the large effect of thermal interactions through the valve module in the current Space Shuttle PLSS.[7] Pressure drops through the system are not modeled.

Radiator

The radiator is the primary heat rejection component in the MPLSS. The design has an aluminum plate to cover the outside of the astronaut's PLSS backpack.[8] A gas gap separates this exterior panel from the water panel, the structure through which water diverted from the WCL flows. The gas gap can be evacuated to impede heat transfer between the water panel and the exterior radiation plate. The water is diverted from the WCL using the radiator's TCV, the control actuator for this component. The radiator model presently consists of three mass nodes, the mass of the water residing in the water panel at any instant in time, the mass of the water panel, and the mass of the exterior gas gap shell. The thermal conductivity of the gas gap varies with gas gap pressure. The gas gap conductance is assumed to be a constant value for this paper.

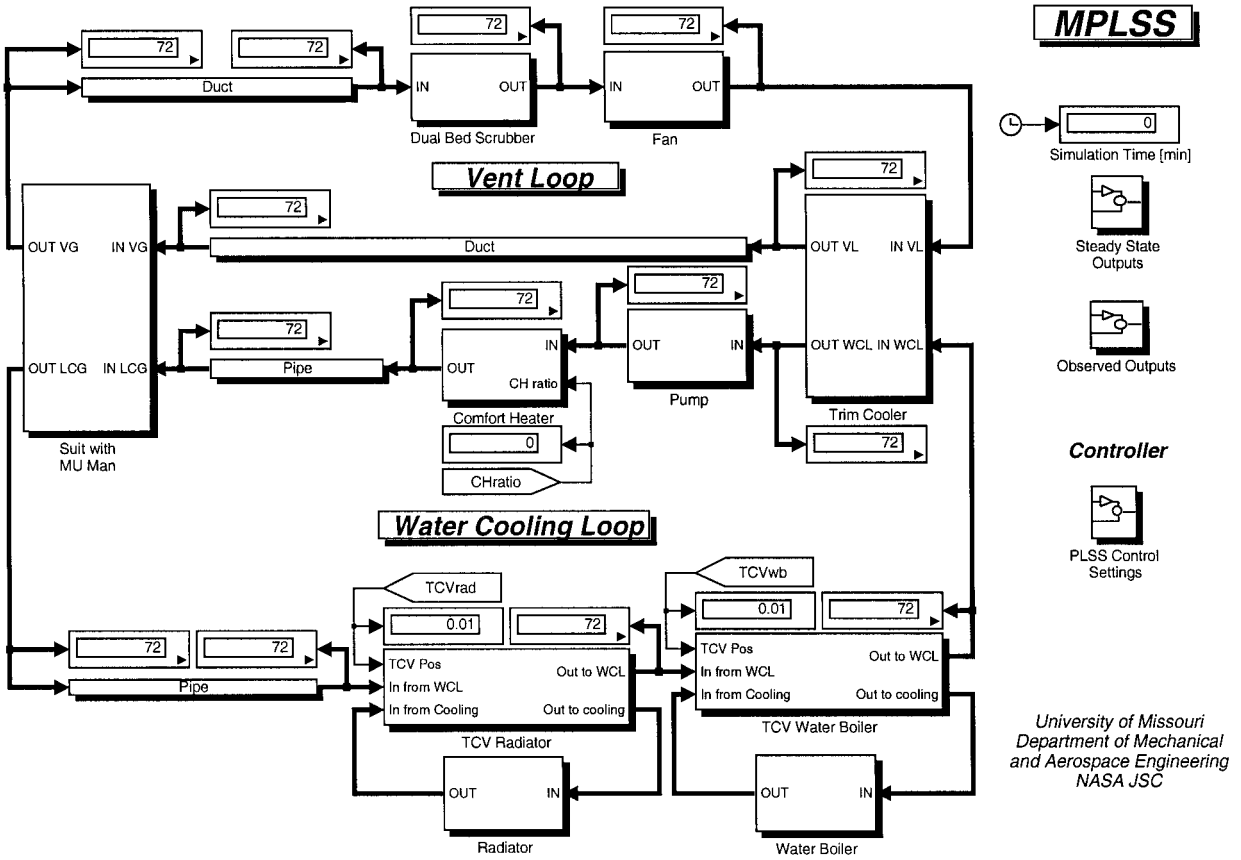

Fig. 3 MPLSS model main window.

The exterior gas gap shell sees heat transfer with the environment via radiation, convection, and solar absorption.

Water Boiler

The water boiler or water membrane evaporator is the secondary cooling unit in the MPLSS and is used when the radiator cooling capacity is insufficient.[1] The cooling is supplied by the evaporation of water to space through a membrane. The water boiler model currently consists of two mass nodes, the mass of water residing in the water boiler at any instant in time and the mass of the water boiler structure. The water temperature is assumed to be the driving force for evaporation of water to space.

TCV

Two TCVs divert water from the primary WCL into the radiator and the water boiler (Fig. 1). The TCVs are modeled as massless components where the flow rate to the cooling component is determined from a command input in percent, 100% indicating full flow through the component.

Trim Cooler

The purpose of the trim cooler is to cool the VL gas after heat is added by the human and the fan. The trim cooler, therefore, interacts directly with the WCL and VL. The trim cooler is modeled with three nodes, one mass node for the resident water in the trim cooler, one mass node for the heat exchanger in the trim cooler, and one massless node for the gas in the trim cooler. Heat transfer occurs between the gas and the heat exchanger, and the heat exchanger and the water. The heat exchanger *UA* values (overall heat exchange rate) are assumed to be constant for constant WCL and VL flow rates.

Pump

The purpose of the pump is to circulate the water in the WCL. Because pressure drops are not modeled, the pump is modeled only as a heat load in the system. The model consists of two mass nodes, one node for the resident water in the pump and one node for the pump structure.

Comfort Heater

The comfort heater was added to the advanced PLSS design to help with the problem of cold discomfort reported by astronauts and to reduce the response time when warmer water is desired by the astronaut. The comfort heater power output varies from 0 to 50 W. The model consists of two mass nodes, one mass node for the resident water in the comfort heater and one mass node for the comfort heater structure.

WCL Pipe

The pipe model is included in the model to account for the movement of water over a relatively large distance in the PLSS. The pipe model consists of two mass nodes, one node for the resident water in the pipe segment and one node for the pipe structure. The fluid transport delay and convection coefficient are calculated based on mass flow rate, pipe diameter, and pipe length.

LCG

The LCG is responsible for primary heat removal from the body. It is a spandex mesh garment with small tubes woven into the mesh. The WCL water flows through these tubes and removes heat from the body. The LCG model is based on the 41-node man model's representation of the LCG.[9] The model consists of a single massless node representing the water in the LCG. The model assumes that the only heat transfer with the LCG is between the skin and the LCG. The sensible heat transfer between the LCG and the suit gas is added directly to the undergarment/skin node heat balance. The LCG is modeled using the effectiveness-NTU (number of thermal units) method for heat exchanger analysis with the assumption that the heat capacitance of the skin is much larger than the heat capacitance of the LCG water. The

change in water temperature through the LCG can then be calculated as

$$(T_{\text{out,lcg}} - T_{\text{in,lcg}}) = (1 - e^{-UA/\dot{m}_{\text{lcg}}c_{p,l}})(\bar{T}_{\text{skin}} - T_{\text{in,lcg}}) \quad (3)$$

where $T_{\text{out,lcg}}$ is the outlet LCG temperature; UA is the overall heat transfer coefficient (defined as a single parameter), UA between the skin and LCG is calculated using an empirical function of inlet LCG temperature, LCG flow rate $\dot{m}_{\text{lcg}}$, and clothing under the LCG[9]; $c_{p,l}$ is the specific heat capacity of the LCG water; and $\bar{T}_{\text{skin}}$ is the weighted average skin temperature of the trunk, arms, and legs. By the manipulation of the temperature difference equation, the outlet LCG temperature is calculated as

$$T_{\text{out,lcg}} = T_{\text{in,lcg}} + (1 - e^{-UA/\dot{m}_{\text{lcg}}c_{p,l}})(\bar{T}_{\text{skin}} - T_{\text{in,lcg}}) \quad (4)$$

The heat transfer to the coolant of the LCG for each human body segment, $q_{\text{lcg},i}$, is calculated as

$$q_{\text{lcg},i} = f_i \dot{m}_{\text{lcg}} c_{p,l}(T_{\text{out,lcg}} - T_{\text{in,lcg}}) \quad (5)$$

where f_i is the percent of flow of coolant in the LCG to each body segment.

Dual Bed Scrubber

The purpose of the dual bed scrubber is to remove carbon dioxide and control humidity in the VL. The carbon dioxide and water vapor are vented to space via a two-stage absorption–desorption process with a solid amine.[10] The model of the dual bed scrubber assumes that the outlet dew point is 4.4°C (40°F) and that there is no net heat transfer with space; it has two nodes, one massless node for the resident gas in the scrubber and one mass node for the scrubber material structure.

Fan

The purpose of the fan is to circulate the gas in the VL. Because pressure drops are not modeled, the fan is modeled only as a heat load in the system, with two nodes, one massless node for the resident gas in the fan and one node for the fan structure.

VL Duct

The duct model is included to account for the movement of gas over a relatively large distance in the PLSS. The duct model consists of two nodes, one massless node for the resident gas and one node for the duct structure. The fluid transport delay and convection coefficient are calculated based on mass flow rate, duct diameter, and duct length.

B. Human Thermal Model

The human thermal model contained within the integrated MPLSS model has been developed at the University of Missouri (MU) and is called MU man. It has two main components, one being the passive thermal system including the solid tissue structure and circulatory system and the other being the active thermal system.

Passive Thermal System

The MU man is a structural derivative of the 41-node man.[9] The human form is subdivided into 10 cylindrical segments (Fig. 4) representing the head, trunk, arms, hands, legs, and feet. These cylinders are partitioned into four concentric shells, each representing a tissue layer with constant properties and temperature. These tissues are the skin, fat, muscle, and core. Heat flow is only radial, making this a one-dimensional lumped parameter model, a common assumption used in other modeling efforts.[11]

The circulatory system is modeled as a single blood pool in constant contact with all other tissue layers; therefore, blood temperature in the model does not vary with location. This assumption, while constituting a weakness of the human thermal model, facilitates development of a model that yields useful results for EVA applications. It is assumed that perfect heat transfer takes place in the capillary beds ($\dot{m}_b c_{p,b}$ is the heat exchange rate, where $\dot{m}_b$ is the local mass flow rate of blood in the capillary bed and $c_{p,b}$ is the specific heat capacity of blood).

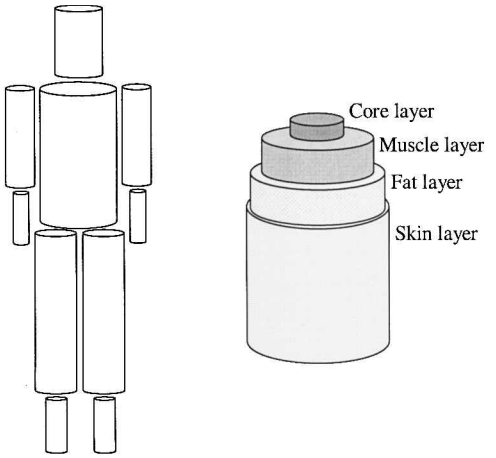

Fig. 4 Human thermal model segmentation and layering.

Energy Balance

There are 10 cylinders each with four layers, and one common blood pool, making it a 41-node model with the general equations shown next. These are solved simultaneously with the MPLSS and suit equations.

Core layer:

$$M_c Cp_c \frac{dT_c}{dt} = \dot{m}_{b\to c} Cp_b(T_b - T_c) + G_{m\leftrightarrow c}(T_m - T_c) + \dot{Q}_{\text{met}} - \dot{Q}_{\text{resp}} \quad (6)$$

Muscle layer:

$$M_m Cp_m \frac{dT_m}{dt} = \dot{m}_{b\to m} Cp_b(T_b - T_m) + G_{c\leftrightarrow m}(T_c - T_m) + G_{f\leftrightarrow m}(T_f - T_m) + \dot{Q}_{\text{met}} - \dot{Q}_{\text{shiv}} - \dot{Q}_{\text{resp}} \quad (7)$$

Fat layer:

$$M_f Cp_f \frac{dT_f}{dt} = \dot{m}_{b\to f} Cp_b(T_b - T_f) + G_{m\leftrightarrow f}(T_m - T_f) + G_{s\leftrightarrow f}(T_s - T_f) + \dot{Q}_{\text{met}} - \dot{Q}_{\text{resp}} \quad (8)$$

Skin layer:

$$M_s Cp_s \frac{dT_s}{dt} = \dot{m}_{b\to s} Cp_b(T_b - T_s) + G_{f\leftrightarrow s}(T_f - T_s) + \dot{Q}_{\text{met}} - \dot{Q}_{\text{lat}} - \dot{Q}_{\text{LCG}} - \dot{Q}_{\text{VG}} - \dot{Q}_{\text{suit}} \quad (9)$$

Blood pool:

$$M_b Cp_b \frac{dT_b}{dt} = Cp_b \sum_{i=1}^{10} \sum_{j=1}^{4} \dot{m}_{b\to i,j}(T_{i,j} - T_b) \quad (10)$$

where M is mass, Cp specific heat, and G the conductance with adjacent nodes.

Active Thermal System

The thermoregulators determine various heat loads and blood flow rates based on the thermal state of the subject. There are four thermoregulators included in the human model: sweating, shivering, vasodilation (increased blood flow to the skin), and vasoconstriction (decreased blood flow to the skin). Both sweating and shivering are heat rates that drive system response and are included in the skin and muscle layer energy balances, respectively. Vasodilation and vasoconstriction affect how quickly heat is transferred from the blood pool into the skin layer. They are modeled as empirical functions of the difference between the actual and setpoint hypothalamus temperatures (approximated by head core) and between the actual and setpoint skin temperatures.

C. Suit and Ventilation Garment

In the terminology used here, suit refers to the thermal and pressure barrier between the astronaut and the environment, and ventilation garment VG refers to the interior of the suit through which gas passes from the helmet over the astronaut and into the ducts located at the wrists and ankles. The flow is split so that 75 and 25% of the flow pass over the arms and legs, respectively.

The suit model consists of 20 mass nodes, 10 interior nodes T_{si}, and 10 exterior nodes T_{so}. Each set of interior and exterior nodes correspond to a cylinder of the human thermal model. The VG consists of 10 massless gas nodes T_g that correspond to the 10 cylinders of the human thermal model. There are five undergarment massless nodes T_{ug} for the torso, arms, and legs, which represent the LCG and TCU fabric. The undergarment temperatures for the head, hands, and feet are equal to the skin temperatures because the LCG does not cover these body segments. A schematic of the thermal model of a suit segment is shown in Fig. 5. Conduction is modeled between the skin and the undergarment for the torso, arms, and legs, and between the suit inner and outer surfaces. Convection is modeled for the gas in the VG with the undergarment/skin and the inner suit surface. Radiation is modeled between the undergarment/skin and the inner suit surface. Convection and radiation between the environment and the exterior surface are modeled such that the exterior environment (temperature, wind speed, and solar flux) can be prescribed to be functions of time.

D. Model Evaluation

The MPLSS design has not been realized in hardware yet, and so the model evaluation is performed by comparing its performance with three steady-state operating points developed by NASA.[1] The NASA steady-state operating points were calculated using simplified overall modeling concepts with low, medium, and high metabolic rates (MRs), in the nominal Martian environment (Table 1). Each operating point was implemented in the MPLSS model, the simulation run to steady state (3 h), and the heat loads and temperatures compared with the operating point values. The fully integrated MPLSS model comparison in Table 2 shows several minor discrepancies between the MPLSS model and the operating points. This reveals the need for an integrated model of the entire system to predict accurately the steady-state heat loads and comfort performance. Numerous interactions have to be considered to predict the human-suit–MPLSS system performance, which cannot be achieved by combining the results of simplified steady-state models.

E. Controller

The thermal control strategy for the MPLSS is much more complicated than the Shuttle PLSS. There are three basic thermal control mechanisms for the MPLSS design: 1) radiator TCV position, 2) water boiler TCV position, and 3) comfort heater power. Because dynamics is the focus of the studies here, a simple controller is implemented to adjust the three control mechanisms to provide thermal comfort and conserve consumables, which are the water

Table 1 Design Martian environments with $P = 8.5$ mbar (0.123 psia)[1]

Environment	Temperature, °C (°F)	Solar flux, W/m^2 (Btu/h-ft^2)	Wind velocity, m/s (ft/s)
Cold	−123 (−189.0)	0 (0)	0 (0)
Nominal	−58 (−72.4)	473 (150)	10 (33)
Warm	−23 (−9.7)	473 (150)	10 (33)
Hot	20 (68.0)	631 (200)	15 (49)

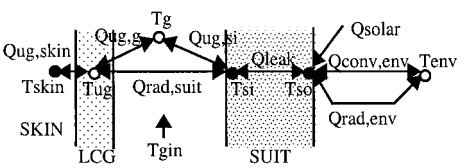

Fig. 5 Suit segment thermal model schematic.

Table 2 Comparison of integrated MPLSS model predictions and steady-state operating points

Operating point (OP)	Q_{stor}, W-h		$T_{in,lcg}$, °C		$T_{out,lcg}$, °C		$T_{in,vg}$, °C		$T_{out,vg}$, °C		$T_{in,dew}$, °C		$T_{out,dew}$, °C		T_{si}, °C		T_{so}, °C		Q_{leak}, W		Q_{lcg}, W		Q_{lat}, W		Q_{rad}, W		Q_{wb}, W	
	Model	Nom.	Model	OP	Model	OP	Model	OP	Model	OP	Model	OP	Model	OP	Model	OP	Model	OP	Model	OP	Model	OP	Model	OP	Model	OP	Model	OP
1[a]	24	5.3	31.46	28.37	31.68	28.88	30.9	27.8	29.2	25.6	4.4	4.4	20.3	16.8	26.7	23.6	−1.67	−2.00	58.0	52.5	23	54	65	45	110	143	6.4	6.2
2[b]	18	15	21.99	22.12	23.57	23.67	21.8	21.8	26.5	24.6	4.4	4.4	19.0	19.0	20.8	20.2	−2.22	−2.33	47.5	46.3	167	164	57	59	157	156	84	84
3[c]	13	24	15.59	16.36	18.39	19.24	15.5	16.2	25.1	23.3	4.4	4.4	19.3	18.7	17.3	17.3	−2.61	−2.67	40.7	41.0	294	305	59	50	141	143	230	239

[a]MR = 150 W, controller settings for radiator TCV, water boiler TCV, and comfort heater input: 7.5, 0.25, and 49.8%.
[b]MR = 275 W, controller settings for radiator TCV, water boiler TCV, and comfort heater input: 97.15, 7.3, and 0%.
[c]MR = 400 W, controller settings for radiator TCV, water boiler TCV, and comfort heater input: 100, 35, and 0%.

expelled through the water boiler and power supplied to the comfort heater. The desired steady-state body heat storage for nominal comfort based on empirical findings[9,12,13] is

$$Q_{\text{nom},ss} = \frac{(\text{MR} - 81)}{3.87}\text{W-h} = \frac{(\text{MR} - 278)}{13.2}\text{Btu} \qquad (11)$$

where MR is the human metabolic rate in watts (or British thermal units per hour) and 81 (278) is the basal MR. The body heat storage should not deviate from $Q_{\text{nom,ss}}$ by more than ±19 W-h (65 Btu). This defines a warm and cold comfort band for the human body. The deviation from nominal body heat storage indicates the body's thermal state and is used by the controller to adjust the comfort heater and TCV settings every 18 s.

III. Design Studies

A. Baseline Performance

The baseline MPLSS performance for the cold, nominal, warm, and hot design environments (Table 1) with low, medium, and high MRs is given in Table 3. To generate Table 3, the various environment and MR situations were prescribed, and the MPLSS controller was allowed to choose the controller settings to bring the astronaut to nominal comfort at steady state (3-h simulation). The comfort value given in Table 3 is the difference between estimated and nominal comfort body heat storage. A comfort value outside of the ±19-W-h (65-Btu) band represents thermal discomfort. The MPLSS provided nominal comfort in all situations except the cold–low, warm–high, and hot–high MR cases. The warm–high MR case maintained thermal comfort with a comfort value of 17 W-h (58 Btu).

The significance of the suit heat leak can be seen in Table 3. The heat leak ranges from 176 to −58 W (599 to −198 Btu/h). The large heat leak in the cold–low metabolic rate case makes providing thermal comfort difficult with the current suit conductance and comfort heater capacity. The heat leak rates for the various conditions can be seen in Fig. 6 as a function of MR and environment. From Fig. 6, it can be seen that heat leak decreases as the environment gets warmer and the MR increases. The MR dependence of the heat leak is explained by the lower LCG and skin temperatures desired for higher MRs. Therefore, at higher MRs, the temperature of the inner suit wall is lower and suit heat leak is less.

B. Parametric Studies

Parametric studies were conducted to investigate how various design variables affect astronaut thermal comfort and to provide some insight into the thermal control issues associated with the MPLSS design. The Martian environment (Table 1) is the condition studied here because it is the most thermally demanding of the possible ISS, lunar, and Martian missions. The interdependence of the design variables are revealed by the integrated MPLSS model, and the need for considering the entire system when making design decisions is demonstrated.

Table 3 Baseline MPLSS steady-state performance for design environments and metabolic rates

Environment	MR, W	Comfort, W-h	Radiator TCV, %	Water boiler TCV, %	Comfort heater input, %	Q_{leak}, W	Q_{rad}, W	Q_{wb}, W	Q_{ch}, W
Cold	150[a]	−23	1	1	100	176	63	18	50
Cold	275	0	5.4	1	0	168	122	16	0
Cold	400	0	100	6.1	0	163	194	63	0
Nominal	150	0	9.7	1	0	53	113	16	0
Nominal	275	0	100	7.5	0	47	156	86	0
Nominal	400	0	100	30	0	42	143	224	0
Warm	150	0	100	5.9	0	14	101	72	0
Warm	275	0	100	16.4	0	8.2	86	193	0
Warm	400	17	100	100	0	4.4	76	315	0
Hot	150	0	1	20	0	−53	−6.2	248	0
Hot	275	0	1	79	0	−58	−8.8	345	0
Hot	400	77	1	100	0	−56	−7.6	390	0

[a]Shivering of 6 W is present at steady state for this operating point.

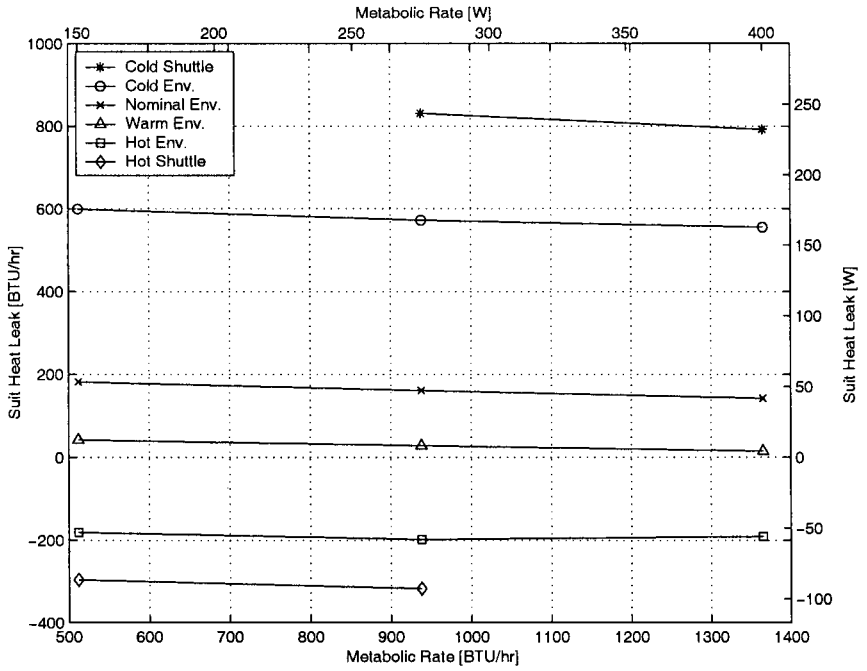

Fig. 6 Baseline design heat leaks along with Shuttle suit conductance heat leaks.

Environmental Limits

The lower environmental temperature limit with the low MR was determined to be −73°C (−100°F) for the baseline MPLSS design to provide nominal comfort for the astronaut. The upper environmental limit for a high metabolic was first investigated in terms of the environmental temperature and then in terms of solar flux. It was determined that for the high MR, the maximum allowable environment is defined by the warm design environment. Therefore, if the MPLSS is to be used for long periods of time, greater than 30 min, in the hot environment with a high MR, the MPLSS design will have to be modified or the astronaut's activity modified to include rest or cool down periods. The MPLSS can provide for astronaut thermal comfort over the entire environmental range for the medium MR.

Suit Conductance

The suit conductance for the advanced MPLSS suit is taken as 0.62 W/m^2-°C (0.11 Btu/h-ft^2-°F), assuming the development of advanced materials.[1] The effect of using a Shuttle-type suit material was investigated, for comparison, by using a suit conductance of 1.19 W/m^2-°C (0.21 Btu/h-ft^2-°F) with the medium and high MRs in the cold Martian environment and the low and medium MRs in the hot Martian environment. The heat leaks with the Shuttle-type suit material can be seen in Fig. 6 compared to the baseline suit material. Comfort was maintained with the Shuttle suit material, but the use of water and comfort heater power increased. In general, a higher suit conductance requires more consumables, with the exception of high MRs in cold environments and low MRs in hot environments, where the increased suit heat leak allows the environment to reduce the PLSS cooling or heating requirement.

The conductance needed to provide thermal comfort in all Martian design environments and design metabolic rates was investigated. It was determined that a conductance value of 0.45 W/m^2-°C (0.08 Btu/h-ft^2-°F) would be sufficient to allow steady-state thermal comfort in the cold environment with the low MR. For the hot environment with the high MR, thermal comfort could not be maintained even with an insulated suit (conductance of 0). Therefore, for the MPLSS to provide for thermal comfort in the hot environment with a high MR, the heat rejection capacity of the water boiler would have to be increased.

Suit Surface Properties

The present baseline design suit has an absorptivity of 0.5 and an emissivity of 0.8, whereas the current Shuttle Suit has an absorptivity of 0.18 and emissivity of 0.837. The increased absorptivity for the baseline design helps to account for surface degradation due to dust and other wear factors. The reduced absorptivity of a Shuttle-type suit material would improve the cooling performance of the MPLSS in the warm and hot thermal environments, reducing the water boiler heat load by as much as 42 W (145 Btu/h). The increased emissivity of the suit would increase cold discomfort in the cold environment and, therefore, increase comfort heater power consumption. Figure 1 shows that the absorbed solar heat flux can be as high as 1037 W (3540 Btu/h) and the radiative heat loss as high as 699 W (2385 Btu/h) indicating that the absorptivity and emissivity of the suit are key design parameters and can greatly affect the cooling requirements for the MPLSS.

Comfort Heater Sizing

The baseline MPLSS design analysis showed that the system could not provide thermal comfort for the astronaut for extended periods of time with a low MR in the cold thermal environment. The maximum comfort heater power is presently 50 W (171 Btu/h). Increasing the comfort heater power to 70 W (239 Btu/h) was enough to provide thermal comfort, within the ±19 W-h (65 Btu) comfort band, for a 3-h simulation, although the body heat storage was decreasing and would eventually go beyond the thermal comfort band. True steady-state comfort is not provided until the comfort heater power is increased to 100 W (341 Btu/h) and nominal comfort is not provided until the comfort heater power is increased to 110 W (375 Btu/h).

Radiator Sizing

Increasing the radiator area to reduce the consumption of water by the water boiler has the undesired result of increasing the heat gain in the hot environments and increasing heat loss in cold environments with low MRs. This tradeoff between desired and undesired heat transfer is quantified via several simulations. In the warm thermal environment with the high MR, the baseline area of 0.65 m^2 (7.0 ft^2) provides marginal comfort by maintaining body heat storage within the ±19 W-h (65 Btu) comfort band, but an increase in radiator area of 57% is necessary to provide nominal comfort. In the hot thermal environment with the high MR, an increase in radiator area of 57% increased the heat absorbed by the radiator by 1.5 W (5 Btu/h) and, therefore, does not have a significant effect on thermal comfort in this situation. In the cold thermal environment with a low MR, an increase in radiator area of 57% increases the heat rejected to space by the radiator by 15 W (51 Btu/h) and causes the astronaut to be even colder in this situation. From this analysis of the tradeoff between desired and undesired radiator heat transfer, it was determined that increasing the radiator area would require increasing the comfort heater power to maintain thermal comfort with a low MR in the cold thermal environment. Because marginal thermal comfort is maintained with the baseline radiator area in the warm thermal environment with the high MR, the added weight and cost associated with increasing the radiator area and with the associated increase in comfort heater power is not justified.

Water Boiler Sizing

In the hot environment with the high MR, it was necessary to increase the water boiler surface area by 60% to provide marginal comfort and 80% to provide nominal comfort; causing an increased water usage (over 3 h of simulation) of 18 and 25%, respectively. In the cold environment with the low MR, increasing the water boiler surface area by 80% only increased the undesired heat transfer by 8% (1 W). Therefore, increasing the water boiler size by 60–80% would help provide thermal comfort in the hot environment with a high MR with the only significant penalties being the increased mass of the unit and the increased water consumption.

WCL Flow Rate

The mass flow rate of the WCL is presently prescribed to be 91 kg/h (200 lbm/h). To study its effect, the flow rate is prescribed to be 50, 75, and 125% of the baseline design value in the warm thermal environment with the high MR and the pump power adjusted using pump similarity rules. The best performance, in terms of thermal comfort, was achieved with the WCL flow rate of 75% baseline (68 kg/h). Increasing the flow rate by 25% from baseline actually decreased the heat transfer to the LCG because the higher flow rate requires a higher pump power, which increases the water temperature and decreases the temperature difference between the LCG water and the skin. In the cold thermal environment with the low MR, decreasing the flow rate by 25% increased cold discomfort for the astronaut due to the decrease in pump power, therefore requiring increased comfort heater power. This tradeoff should be beneficial because the pump power reduction would reduce power consumption and water usage throughout the operating envelope whereas the increased comfort heater power would only effect the cold environment with low MR portions of the operating envelope.

IV. Operating Envelope and System Dynamics

The steady-state baseline MPLSS operating envelope is shown in Fig. 7 in terms of MR and thermal environment. The baseline MPLSS performance showed that the present design cannot maintain thermal comfort in the cold environment with the low MR for more than 90 min and in the hot environment with the high MR for more than 28 min.

To demonstrate how the MPLSS would behave for a typical mission that sometimes moves outside the steady-state operating envelope, the design metabolic and environment profiles (Fig. 2) developed by the Advanced Space Suit Project Group at NASA Johnson

Space Center were implemented using the MPLSS model. The body heat storage and desired body heat storage for nominal comfort are plotted in Fig. 8. A basic controller for the MPLSS is able to maintain thermal comfort for the majority of the simulation. The astronaut does get hot for a short period of time following the two 600-W (2047-Btu/h) spikes, but the MPLSS design does maintain a reasonable level thermal comfort in a demanding mission profile. The analytical aspects of the dynamics of the human-suit–MPLSS system are now discussed including linearized models to further characterize the complex system.

A. Human–Suit Dynamics

The general nonlinear expression for body heat storage is

$$Q_{\text{stor}} = f(\text{MR}, T_{\text{in,lcg}}, T_{\text{in,vg}}, T_{\text{in,dew}}, T_{\text{so}}, t) \tag{12}$$

Linearizing the body heat storage expression about an operating point and neglecting small terms, the change in body heat storage can be expressed, in transfer function form, as

$$\Delta Q_{\text{stor}}(s) \cong P_1(s)\Delta T_{\text{in,lcg}}(s) + P_2(s)\Delta\text{MR}(s) + P_3(s)\Delta T_{\text{so,av}}(s) \tag{13}$$

where

$$P_i(s) = e^{-\tau_{d_i}^s} K_i/(1 + \tau_i s) \tag{14}$$

The following range of operating conditions were selected for the linearizations: 16.1–33.9°C (61–93°F) for $T_{\text{in,lcg}}$, 87.5–462.5 W (299–1578 Btu/h) for MR, and −73.3–60.0°C (−100–140°F) for $T_{\text{so,av}}$. Brief excursions out of the MR operating range are expected during EVA (Fig. 2). Equation (13) is not parameterized for these cases due to the onset of physical impairment at steady state [$|Q_{\text{stor}}| > 88$ W-h (300 Btu) ⇒ physical impairment]. The simulations showed that the transport delay τ_{di} was negligible for the body heat storage. Figure 9 shows three slices of the steady-state operating envelope for the human. Regions of steady-state shivering and sweating are identified illustrating the existence of zones where heat transfer mechanism switching occurs, making the system inherently nonlinear. This nonlinearity is exhibited by the behavior of the system's linearized parameters of Table 4. The large range of system parameters is related to the complexity of the human model including the behavior of its thermoregulators (shivering, sweating, vasodilation, and vasoconstriction) along with the nonlinear nature of several modes of heat transfer such as radiation and evaporation. The parameterizations show that the body heat storage responds slowly to changes in the three inputs. Many other variables of the body, such as mean skin temperature or heart rate, have faster response times to changes in LCG water temperature, activity, or environment.

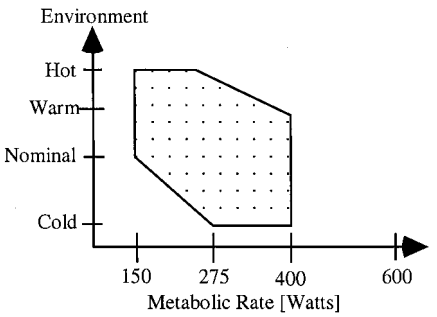

Fig. 7 Steady-state baseline MPLSS operating envelope.

B. MPLSS Dynamics

The response of the MPLSS is discussed in terms of its time constant and 5% settling time.[14] The MPLSS output $T_{\text{in,lcg}}$ (the controlled variable) exhibits higher-order behavior to changes in water boiler and radiator TCV position inputs due to the nonlinearity of the WCL flow being diverted to the water boiler or radiator and then being returned to the primary WCL circuit. To a step change in LCG outlet temperature (inlet to PLSS), with the radiator, water boiler, and comfort heater off, $T_{\text{in,lcg}}$ exhibited a time constant of 1.1 min and a settling time of 2.7 min due to the thermal capacitance of the components that the water interacts with as it circulates through the WCL.

Table 4 Human linearization time constants and gains

Value	τ_1, min	K_1, W-h/°C	τ_2, min	K_2, W-h/W	τ_3, min	K_3, W-h/°C
Average	54.8	144	52.6	9.38	65.4	8.97
Maximum	116	253	91	15.7	97	14.1
Minimum	32	40.5	27	5.46	39	3.69

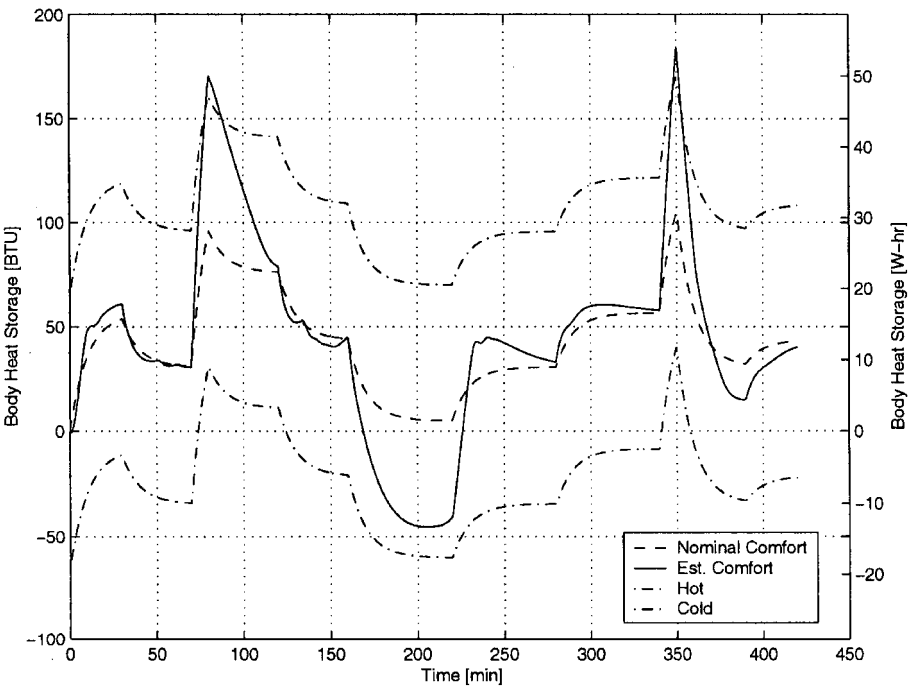

Fig. 8 Body heat storage for controlled MPLSS with design profile.

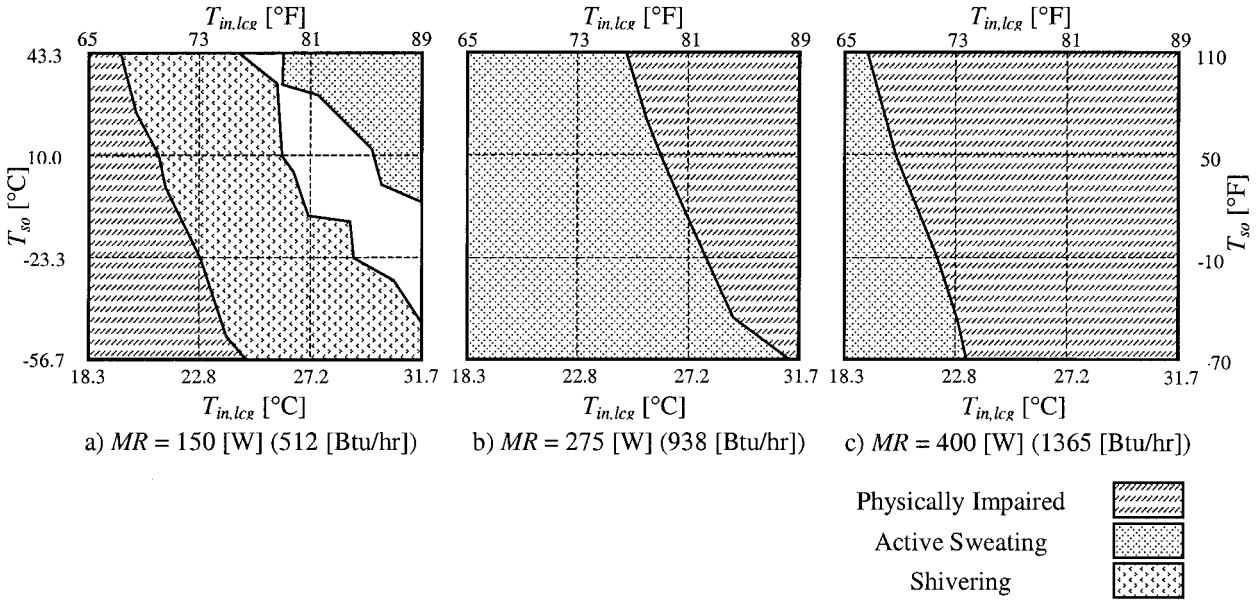

Fig. 9 Examples of steady-state human operating envelope.

A set of open-loop simulations were run with the MPLSS portion of the model, in the nominal thermal environment (Table 1), to determine the response characteristics of $T_{in,lcg}$, the controlled variable, to changes in the three control inputs. The radiator TCV, water boiler TCV, and comfort heater input were each independently changed from minimum to maximum and then from maximum to minimum while the other two control inputs were at their constant, minimum value. The radiator TCV changes resulted in the slowest response with a time constant of 2.8 min and settling time of 9.7 min going from minimum to maximum cooling and a time constant of 10.9 min and settling time of 32 min going from maximum to minimum cooling. The output $T_{in,lcg}$ responded very quickly to water boiler and comfort heater inputs with time constants less than 1 min and settling time less than 2 min. The radiator and comfort heater response times are not sensitive to the outlet LCG temperature prescribed, but the water boiler response times are because water temperature affects the evaporation of water to the environment. The slower response of the system when decreasing the water boiler and radiator TCV positions is due to the decreased flow through the component that decreases the convection between the WCL and the component. Whereas the response times were insensitive to LCG outlet temperatures, the results did indicate the cooling performance of the radiator and water boiler are sensitive to LCG outlet temperature. The radiator provided 19% more cooling and the water boiler provided 50% more cooling when the MPLSS inlet water temperature was increased by 21% from 70 to 85°F for the nominal thermal environment of Table 1.

The radiator is the primary heat-rejection component in the MPLSS in the nominal thermal environment (Fig. 1). It responds slower than the water boiler but is still fast when compared to the human. More cooling is provided as the radiator TCV position is increased. Also, the higher the inlet radiator temperature and the lower the radiator shell temperature are, the greater the heat rejection capacity of the radiator varying with the fourth-order dependence from radiative heat transfer. The water boiler component responds quickly when compared to the human thermal response and to the radiator. More cooling is provided by the water boiler as the TCV position is increased. Also, the higher the inlet water boiler temperature is, the greater the heat rejection capacity of the water boiler, due to the exponential dependence of water vapor pressure on temperature.

V. Results and Discussion

The complexities of the human-suit-MPLSS thermal dynamics are such that a fully integrated model is needed for system and control design. Whereas a steady-state model of the system should allow for preliminary component sizing, a fully integrated transient model of the entire system is needed for detailed design and to evaluate thermal comfort especially with the wide variations in environment (−123–20°C) (−190–70°F) and frequent changes in MR (80–600 W) (273–2046 Btu/h). The complexity of switching human thermoregulatory mechanisms (sweating, shivering, and vasodilation or vasoconstriction) and nonlinearities of the water boiler and radiator need to be understood dynamically to evaluate issues such as duration limits for thermal comfort and operational remedies to cold and warm discomfort problems, as in donning or doffing of an outer garment and rest or exercise periods in extreme environments.

The importance of thermally modeling the various components in the MPLSS can be partly gauged from their heat loads (Fig. 1) and time constants. The most significant component in the overall system is the human because the objective is to keep the human thermally comfortable. The suit must be modeled accurately due to its intimate interaction with the human and the large heat loads from the environment. Even though the water boiler and radiator respond 3–10 times faster than the human, they are both significant due to their large heat loads. These have all been illustrated in the study.

The MPLSS operating envelope (Fig. 7) shows the area of possible MRs and environments in which the MPLSS can provide steady-state or long-term comfort. Operational restrictions could be used to allow short excursions outside of the operating envelope. As an example, in the cold environment, the restriction could be to not allow the low MR for over 1 h without some high MR warm-up period. Techniques, such as an additional outer garment to provide an increased impedance to heat leaks to the environment, could also be employed to extend the time allowed for the low MR, cold environment condition.

The parametric design studies showed the suit material and surface properties to be significant design parameters with the result that increasing the isolation of the astronaut from the environment increases the thermal comfort of the astronaut in extreme situations (hot–high MR and cold–low MR). Increased thermal isolation from the environment decreases consumable usage in extreme situations but may reduce desired heat leaks through the suit in moderate conditions, which would, therefore, increase consumable usage. The minimum water flow rate required through the radiator and water boiler to resist freezing causes unwanted heat rejection to space in the cold environment and, therefore, increases cold discomfort. The comfort heater analysis showed that the comfort heater power must be increased by 40–120% to provide thermal comfort in the cold environment with the low MR. The radiator area analysis showed

that the added benefit of a larger radiator did not outweigh the costs in terms of increased comfort heater requirements and weight. The water boiler analysis showed that increasing the water boiler surface area by 60–80% would allow for the MPLSS to provide comfort in the hot environment with the high MR. The analysis of the WCL flow rate showed that decreasing the WCL flow rate by 25% would decrease the pump power requirement and still allow sufficient cooling by the LCG with the only penalty being an increase in comfort heater capacity.

Design of the next generation space suit requires balancing the competing objectives for a set of complex systems to arrive at a final system design that will provide thermal comfort in the largest set of scenarios with the minimum use of consumables. The basic tradeoff seen in each of the design studies is the tradeoff between performance (in terms of thermal comfort, speed of response, comfort envelope, and efficiency of mission) and cost (in terms of consumables, mass, and volume). The present baseline design balances these competing factors well. Some extreme cases can also be accommodated by ideas such as the donning and doffing of a parka-type garment to decrease heat transfer with the environment, placing upper limits on the MR allowed in a hot environment and lower limits in cold environments, required cool-down periods and duration limits in hot environments with high MRs, and required warm-up periods and duration limits in cold environments with low MRs. The dynamic MPLSS model used in this study can be used to effectively study such scenarios, which are required before a detailed thermal design is finalized.[7]

The response times reported in the preceding section show that the MPLSS is 3–10 times faster than the human. The dynamic characteristics and reduced-order models will be utilized for control design studies.

VI. Conclusions

Thermal modeling and dynamic design issues have been reported for a complex space suit system, after an overview of the thermal technologies involved. To design the space suit system and provide optimal thermal comfort, an integrated dynamic simulation testbed is required. Such a transient testbed of the MPLSS advanced space suit design has been developed including the human thermal dynamics. The model has been developed to help with sizing and evaluation of the MPLSS design, as well as aid in the development and evaluation of an automatic thermal comfort control strategy. The modularity and flexibility of the MPLSS model facilitates rapid studies of alternative designs, modifications, and technologies. As prototype components are developed and tested, experimental experience can also be incorporated into the MPLSS model. Operational investigations can also be conducted to investigate the cost and benefits of donning and doffing an outer garment, exercise and rest periods in extreme environments, and duration limits for activity levels in extreme environments. The testbed simulation can also be used for thermal comfort controller design and evaluation.

Acknowledgment

The reported work was supported in part by NASA Johnson Space Center Grant NAG-9-915.

References

[1]Lawson, M., Cross, C., and Stinson, R., "The Advanced Space Suit Project—97 Update," Society of Automotive Engineers, Paper 981629, July 1998.

[2]Cross, C., and Chipwadia, K., "Advanced Technology Spacesuit Technical Requirements Document," NASA Johnson Space Center, JSC Document 38715, Houston, TX, 1997.

[3]Campbell, A. B., Nair, S. S., Miles, J. B., and Webbon, B. W., "PLSS Transient Thermal Modeling for Control," *Journal of Aerospace*, Vol. 105, No. 1, 1996, pp. 675–684.

[4]McBarron, J. W., II, Whitsett, E. E., Severin, G. I., and Abramov, I. P., "Individual Systems for Crewmember Life Support and Extravehicular Activity," *Space Biology and Medicine*, AIAA, Washington, DC, 1991, pp. 275–330.

[5]Portee, D. S. F., and Trevino, R. C., "Walking to Olympus: An EVA Chronology," *Monographs in Aerospace History Series #7*, NASA History Office, 1997.

[6]Mays, D. C., French, J., Nair, S. S., Miles, J. B., and Lin, C. H., "Design of a Transient Thermal Model of the Cryogenic PLSS," Society of Automotive Engineers, Paper 1999-01-2000, July 1999.

[7]Campbell, A. B., "Thermal Modeling, Analysis, and Control of a Space Suit," Ph.D. Dissertation, Dept. of Mechanical and Aerospace Engineering, Univ. of Missouri, Columbia, MO, Aug. 1999.

[8]Cross, C., Trevino, L., and Laubach, J. G., "Thermal Performance of the Radiator Advanced Demonstrator," Society of Automotive Engineers, Paper 981672, July 1998.

[9]Bue, G. C., "Computer Program Documentation 41-Node Transient Metabolic Man Program," NASA Johnson Space Center, CTSD-0425, Houston, TX, 1989.

[10]Filburn, T., Dean, W. C., and Thomas, G., "Development of a Prototype Pressure Swing CO2/H2O Removal System for an Advanced Spacesuit," Society of Automotive Engineers, Paper 981673, July 1998.

[11]Wissler, E. H., "Mathematical Simulation of Human Thermal Behavior Using Whole Body Models," *Heat Transfer in Medicine and Biology*, edited by A. Shitzer and R. C. Eberhart, Vol. 1, Plenum, New York, 1985, pp. 325–373.

[12]Waligora, J. M., "Thermal Comfort and Tolerance Design Criteria," NASA TM-84849, 1967.

[13]Dunaway, B., "Automatic Liquid and Ventilation Cooling Garment Control Algorithm Final Test Report," NASA Johnson Space Center, JSC CTSD-SS-176, Houston, TX, 1987.

[14]Franklin, F. F., Powell, J. D., and Emami-Naeini, A., *Feedback Control of Dynamic Systems*, 3rd ed., Addison–Wesley, Reading, MA, 1994.